Available online at www.sciencedirect.com
ScienceDirect
Metamaterials 3 (2009) 140–147
Metamaterials
www.elsevier.com/locate/metmat

3D isotropic metamaterial based on a regular array of resonant dielectric spherical inclusions

I.B. Vendik, M.A. Odit *, D.S. Kozlov

St. Petersburg Electrotechnical University, 5 Prof. Popov Str., St. Petersburg 197376, Russia

Received 17 April 2009; received in revised form 28 August 2009; accepted 7 September 2009
Available online 30 September 2009

Abstract

The 3D regular lattice of bi-spherical dielectric resonant inclusions arranged in a cubic lattice as two sets of dielectric spheres having different radii and embedded in a host dielectric material with lower dielectric permittivity was carefully investigated. The magnetic resonance mode in smaller spheres gives rise to the magnetic dipole momentum and the electric resonance mode in bigger spheres is responsible for the electric dipole momentum. The magnetic resonance corresponding to the first Mie resonance in the spherical particles is followed by forming a regular array of effective magnetic dipoles, and the structure of the identical spherical dielectric resonators can be designed as an isotropic μ-negative 3D-metamaterial. At the same time, it was found experimentally and by the simulation that the resonant response of the electric dipole was weakly pronounced and the ε-negative behavior was remarkably suppressed. To enhance the electric dipole contribution, two different ways were considered: (i) using another kind of symmetry of the bi-spherical arrangement of the particles corresponding to the body-centered cubic symmetry instead of the symmetry of NaCl analog considered previously; (ii) using a strong coupling between the identical resonant dielectric spheres arranged in the simple cubic symmetry for creation of the structure exhibiting properties of the isotropic DNG medium.

PACS: 94.20.ws; 78.20.Ci; 41.20.Jb; 94.05.Pt

Keywords: Metamaterial; Resonant inclusion; Mie resonance; Magnetic dipole; Electric dipole; Isotropic; Backward wave

1. Introduction

Medium with simultaneously negative permittivity and permeability or so-called double negative medium (DNG) can be formed by a regular lattice of inclusions considered as artificial "molecules". In many practical cases, isotropic DNG structure is very attractive. Different ways to create the 3D isotropic DNG medium have been suggested [1–11]. The structure is designed as a regular array of cubic or spherical inclusions. Using a cubic arrangement with split-ring resonators on the faces and a wire medium was suggested and discussed in [1–3]. Another way is to use intrinsic properties of the inclusions, in particular plasmonic nanoparticles to design metamaterial for optical frequency range [4,5]. The isotropic DNG structure for microwave applications can be designed as a regular lattice of resonant dielectric inclusions, providing excitation of electric and magnetic dipoles. These dipoles form the artificial medium exhibiting DNG behavior in a limited frequency range near the resonant frequencies. Dielectric disk, cylindrical, or spherical resonators are suitable for establishing the dipole moments. Metamaterials with desired values

* Corresponding author. Tel.: +7 812 346 0867; fax: +7 812 346 0867.
E-mail address: maodit@mail.eltech.ru (M.A. Odit).

1873-1988/$ – see front matter © 2009 Elsevier B.V. All rights reserved.
doi:10.1016/j.metmat.2009.09.001

of permeability $\pm\mu$ and permittivity $\pm\varepsilon$ are developed by exciting electric and magnetic resonant modes [6–12]. The 3D regular lattice of bi-spherical dielectric resonant inclusions was suggested for the first time in [7,8]. In this structure, the metamaterial medium is composed of two sets of spherical particles made from the same dielectric material embedded in a host dielectric material. The spheres differ by radius. The dielectric constant of the spherical particles is much larger than that of the host material. By combining two sets of the spheres with suitable radii, different modes can be simultaneously exited in the spheres: the magnetic resonance mode giving rise to the magnetic dipole momentum and the electric resonance mode being responsible for the electric dipole momentum. In [8–10], it was suggested that the dielectric resonators do not interact and for the 3D structure the responses of both the spherical particles are superimposed. By full-wave simulation and experimental investigation, it was found that the resonance response of the magnetic dipole is very effective and the μ-negative isotropic metamaterial can be designed as a regular array of dielectric spherical particles with the first Mie resonance. At the same time, the electric dipole corresponding to electric resonance mode is weakly pronounced. As a consequence, the ε-negative behavior is blurred [10].

Detailed theoretical description based on full-wave analysis was performed in [12] for different all-dielectric structures of metamaterial: single-negative (SN) medium based on the spherical particles; bi-spherical DNG medium on an array of the dielectric spherical particles of the same radius made from two materials differing in dielectric permittivity; a set of identical discs and discs made of two different dielectric materials etc. The last structures based on the discs form 2D SN and DNG metamaterials. Interesting 2D structures based on cylindrical resonator arrays situated in a parallel-plate waveguide have been discussed and experimentally verified in [13,14]. In these structures, the DNG properties are provided by magnetic resonance in the cylinders (magnetic dipole, μ-negative behavior) and by ε-negative response of electromagnetic wave in a parallel-plate metallic waveguide with TE_n modes below the cut-off frequency.

Recently the experimental investigation of isotropic metamaterials based on resonant dielectric inclusions has been reported [15–17]. The resonant μ-negative response was registered in the 3D structure based on a regular array of dielectric cubes in [15] and the 2D array of cubes in [16]. The 3D DNG material was realized as a set of dielectric spherical particles regularly distributed in a metallic wire frame exhibiting cubic symmetry. The wire frame provides an environment with evanescent waves followed by effective negative permittivity, which in combination with the resonant dielectric particles giving rise to magnetic dipole and negative permeability leads to a propagating wave with negative phase velocity, i.e. forms the 3D isotropic DNG medium.

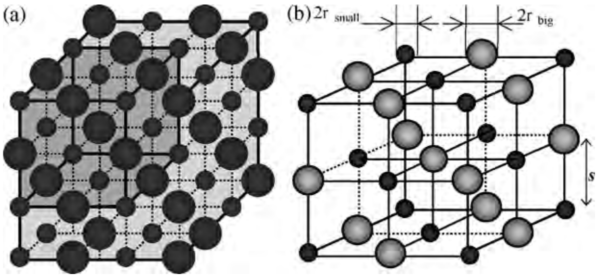

Fig. 1. (a) Bi-spherical NaCl-like structure with two types of resonators. (b) Single cell of the NaCl-like structure.

All these achievements support the fruitful idea of a realization of the isotropic metamaterial using dielectric resonant inclusions. In order to improve the performance of the all-dielectric DNG medium with cubic symmetry based on spherical dielectric particles, we suggest the new structures obtained by: (i) changing the symmetry of the single cell of the bi-spherical structure to enhance the contribution of the electric resonance in the effective dielectric permittivity; (ii) to use strongly coupled resonant dielectric spherical particles arranged in a simple cubic symmetry, when the magnetic dipole is originated inside the spheres, whereas the electric dipole arises from the electrical coupling between the spheres.

In this paper, we consider both the approaches: the 3D DNG bi-spherical structure based on the single cell exhibiting the body-centered cubic symmetry and the medium formed by strongly coupled spherical resonant inclusions.

2. 3D isotropic bi-spherical metamaterial of cubic symmetry with high packing density

Let us consider two sets of the spherical particles arranged in the NaCl-like structure (Fig. 1a). This structure has face-centered cubic lattice and is a member of the cubic system of symmetry pertaining to the class $m3m$ [8,18]. In the case of cubic symmetry, the second rank tensors of all physical parameters of the media are diagonal and have the components of the same values [18]. Thus the permittivity and permeability tensors are written in the following form:

$$\varepsilon = \begin{vmatrix} \varepsilon_{eff} & 0 & 0 \\ 0 & \varepsilon_{eff} & 0 \\ 0 & 0 & \varepsilon_{eff} \end{vmatrix},$$

$$\mu = \begin{vmatrix} \mu_{eff} & 0 & 0 \\ 0 & \mu_{eff} & 0 \\ 0 & 0 & \mu_{eff} \end{vmatrix}, \quad (1)$$

where the sub-indices *eff* are introduced to stress that the permittivity and permeability are obtained as a result of averaging electric and magnetic polarization of spherical particles embedded in the matrix. The result of averaging the polarization of the spherical particles depends on the volume of the matrix falling on each particle considered. Body-centered and face-centered structures are related to the same class of symmetry and by the same form of the second rank tensor as the simple cubic structure. These structures are characterized by a higher packing density as compared with the simple cubic structure.

A low-level cell of the structure (Fig. 1b) contains 4 particles of each kind. The distance between the two adjacent resonators is marked as s, while the distance between the resonators of the same radius (as well as the cell size) is $2s$. The volume fraction of the particle of radius r in the cell is defined by equation:

$$v_f = 4\frac{(4/3)\pi r^3}{(2s)^3} \quad (2)$$

Simulations revealed that the particles should be placed as close as possible to each other in order to strengthen the DNG effect. At the same time a high density of the particles is followed by their mutual interaction and, as a consequence, shifting resonances and their distortion.

In order to get an optimal distance between the resonant particles and at the same time to keep the $m3m$ symmetry of the structure, the body-centered structure was introduced. A low-level cell of this structure is depicted in Fig. 2. Here the single cell contains 1 particle of each kind, but the distance between the same particles is s, while in case of face-centered structure this distance is equal to $2s$. At the same time the distance between the adjacent particles (of different kind) is equal to $(1/2)s\sqrt{3}$. In this case the volume fraction of the particles is two times higher than for the face-centered structure. The volume fraction for the resonator is

$$v_f = \frac{(4/3)\pi r^3}{s^3} \quad (3)$$

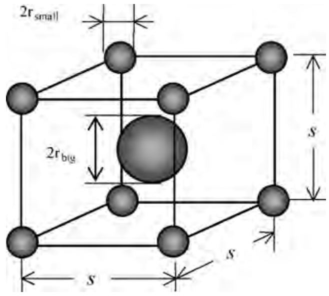

Fig. 2. Body-centered single cell.

At the same time, the distance between the adjacent particles is still big enough to neglect the effect of their interaction.

The effective electromagnetic parameters of the bi-spherical array have been analytically found by solving the problem of diffraction of the plane wave on the non-interacting dielectric spheres [9]. For two different structures, the frequency dependent effective permittivity and permeability were calculated in the same way (Eqs. (4) and (5)):

$$\varepsilon_r^{(eff)}(f) = \frac{n}{s^3}\varepsilon_p \frac{3}{2} I_1(f) \cdot b^{(t)}(f, r_{big}) + \varepsilon_h, \quad (4)$$

$$\mu_r^{(eff)}(f) = \frac{n}{s^3}\sqrt{\frac{\varepsilon_p}{\varepsilon_h}}\frac{3}{2} I_2(f) \cdot a^{(t)}(f, r_{small}) + \mu_h \quad (5)$$

Here s is the distance between the adjacent particles (see Figs 1b and 2), ε_p (μ_p), ε_h (μ_h) are the permittivity (permeability) of the particle and the host material respectively, r_{small} and r_{big} are the radii of the resonators, f is the incident electromagnetic wave frequency, $a^{(t)}$ and $b^{(t)}$ are the amplitudes of spherical wave functions, F_{eps} and F_{mu} are the results of integration of the electric and magnetic field components over the particle volume [9,10], $n = 0.5$ for the NaCl-like structure and $n = 0.65$ for the face-centered structure. $I_1 = -22.4 \times 10^{-20}\ f + 2.2.5 \times 10^{-9}$ and $I_2 = -10.64 \times 10^{-20}\ f + 1.42 \times 10^{-9}$ are approximate functions in the frequency region f = 9.99–10.02 GHz.

In case of the body-centered lattice the value of the effective parameters ε and μ at the resonance is approximately two times higher as compared with the face-centered lattice. In Fig. 3, the results of calculation of the effective parameters of the bi-spherical metamaterial are presented for two different structures with parameters: $\varepsilon_p = 400$, $\varepsilon_h = 1$, $\mu_\mathrm{p} = \mu_h = 1$, $r_{small} = 0.748$ mm and $r_{big} = 1.069$ mm, the loss factor of the dielectric material of the particles was taken $\tan\delta = 0.001$. The host dielectric was suggested to be lossless. Evidently the response of the body-centered lattice is higher than that of the face-centered lattice.

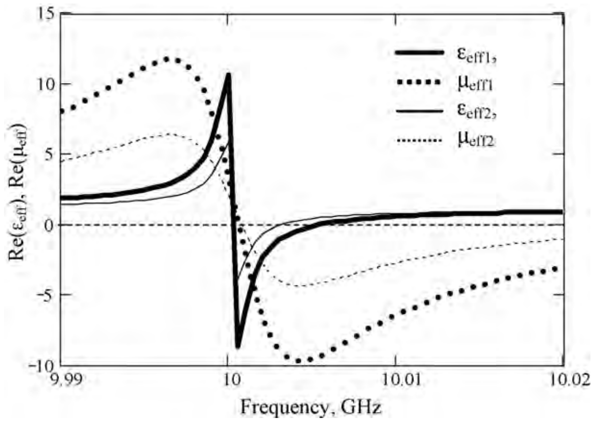

Fig. 3. Effective permittivity and permeability for the body-centered (sub-index 1) and face-centered (sub-index 2) structures.

Analysis of the influence of the loss factor of the dielectric material $\tan\delta$ on the effective parameters revealed that there is no remarkable change in the effective parameter values for $\tan\delta \le 0.003$ [9]. As a suitable dielectric material for the resonant spherical inclusions ceramics $BaO–SrO–Nd_2O_3–TiO_2$ can be used; this material demonstrated $\varepsilon_r = 400$ and $\tan\delta \le 0.003$ in microwave region [19].

In order to confirm the effectiveness of the body-centered lattice, let us consider the simplified case of limited in one direction structure (Fig. 4) using full-wave analysis. Due to the translation symmetry, the structure is bounded by perfect electric conductor (PEC) and perfect magnetic conductor (PMC). The structure contains 7 single cells along the wave propagation direction. The single cell is centered by the spherical particle of a bigger value of the radius r_{big} ($r_{big} = 1.05$ mm) and is surrounded by the particles of a smaller value of the radius r_{smal} (0.748 mm). The distance between the particles of the same size is $s = 4$ mm. The particle dimensions are chosen to provide the magnetic resonance in the smaller spheres and the electric resonance in the bigger particles at the same frequency. It results in creation of magnetic and electric dipoles followed by the negative effective permeability and effective permittivity in a limited frequency range. That leads to appearance of transmission of electromagnetic wave in this frequency range (Fig. 5). The full-wave analysis of the electromagnetic wave propagation confirms existence of the backward wave. In Fig. 6 the magnetic field pattern is shown for four different moments of the period of time. It is clearly seen that the wave propagates from the right side to the left, whereas the incident wave enters the structure from the left side.

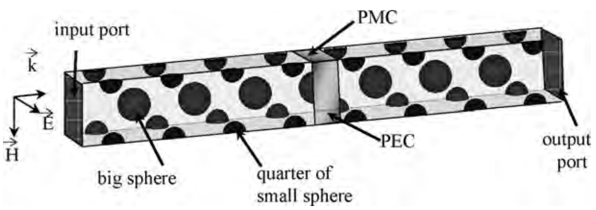

Fig. 4. One-dimensional structure of bi-spherical isotropic metamaterial. Radii of small and big spheres are 0.748 mm and 1.05 mm, respectively. Boundary conditions are provided by perfect magnetic (PMC) and perfect electric (PEC) walls.

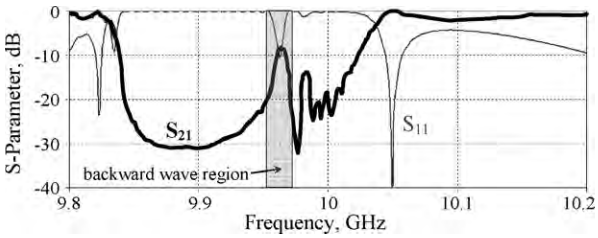

Fig. 5. Transmission S_{21} and reflection S_{11} coefficients for the structure depicted in Fig. 3. Gray area is the frequency range, where the resonant frequencies of the two types of resonances coincide and backward wave is observed.

The 3D volumetric structure is shown in Fig. 7. The small and big spherical particles are situated in different planes. The same is related to the magnetic and electric dipoles. The PECs and PMCs are used for providing boundary conditions for this limited in volume structure. The dimensions of the spherical particles and spacing between the identical particles are the same as in the previous case (Fig. 4). Magnetic field pattern for the section plane shown in yellow in Fig. 7a is depicted in Fig. 7b for four different moments of the time period. Again the backward wave is observed. The response of the structure to the incident plane electromagnetic wave is presented in Fig. 8. In the limited frequency range one can observe

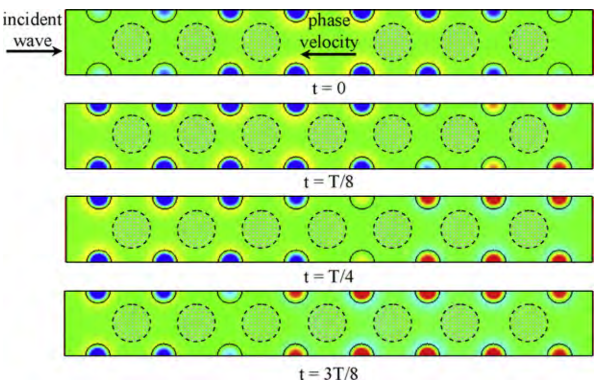

Fig. 6. Magnetic field patterns for four different moments of the period of time. The incident wave enters the structure from the left side, whereas the wave inside structure propagates from the right to the left side.

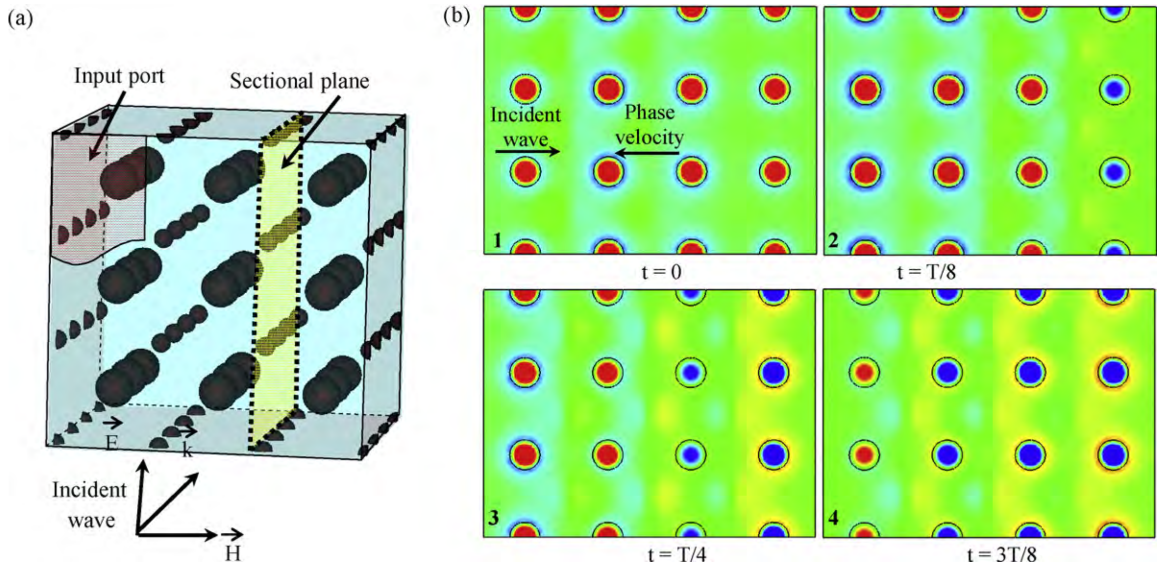

Fig. 7. (a) Bi-spherical structure of metamaterial with body-centered cubic symmetry. Radii of small and big spheres are 0.748 mm and 1.05 mm, respectively. Distance between the same particles is 4 mm. (b) Magnetic field patterns for the section plane shown in yellow in (a) for 4 different moments of the period of time.

the wave transmitting through the DNG structure. It is important to stress that the frequency range of the DNG behavior is shifted to the higher frequencies as compared with the characteristic of the structure of Fig. 4. This effect can be explained by coupling of the spherical particles in real volumetric structures, which was not taken into consideration by the analytical description of the electromagnetic wave diffraction on the single spheres, but was highlighted by the full-wave analysis. In general, the effect of the backward wave propagation is confirmed.

3. 3D-metamaterial based on a regular array of strongly coupled dielectric spherical resonators

When the spacing between the adjacent dielectric spherical resonators is small, they interact and influence each other. The coupling between the resonators leads to forming new electromagnetic field distribution in the

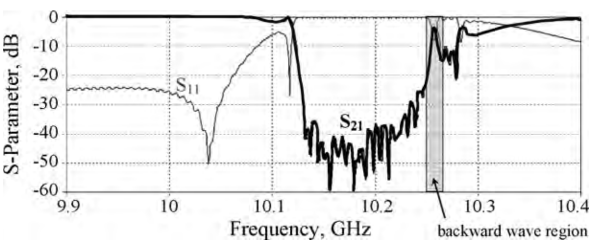

Fig. 8. Transmission S_{21} and reflection S_{11} coefficients for the modeled structure depicted in Fig. 5. Gray area is the frequency range where the two types of resonances coincide and backward wave is observed.

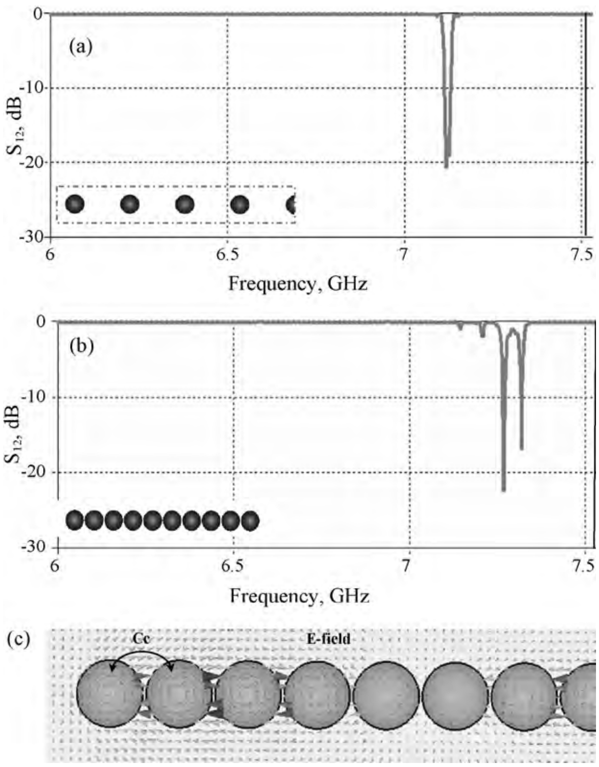

Fig. 9. Transmission coefficient of 1D structure of distantly positioned non-coupling (a) and close positioned coupling (b) resonators. Electrical field between coupled resonators (c).

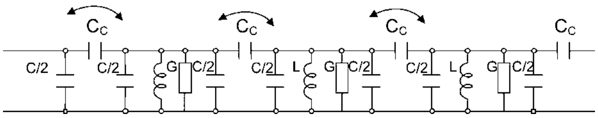

Fig. 10. Equivalent circuit of coupled parallel tanks.

medium outside the spheres. That makes it possible to observe electric and magnetic dipole response: magnetic dipole comes from the first Mie resonance in the dielectric sphere, and the electric dipole is formed by the sphere interaction conditioned by the electric field outside the sphere surface. Electric and magnetic dipole existence provides double negative response of the media.

The 1D regular structure of the spherical particles is shown in Fig. 9. If the spacing is large enough, i.e. more than the sphere diameter, there is no remarkable interaction between the adjacent spheres. For the distantly positioned spheres, the resonant stop-band is observed at the resonant frequency of the magnetic mode (Fig. 9a). By decreasing the spacing between the spheres, the splitting of the resonance characteristic occurs and a pass band appears near the resonant frequency (Fig. 9b). The electric field distribution responsible for electric coupling is shown in Fig. 9c.

The one-dimensional case of coupled resonant dielectric spheres can be considered as the dual analog of magneto-inductive waveguide [20,21] described by an equivalent circuit of magnetically coupled series resonant tanks. In our case the 1D structure can be presented by electrically coupled parallel tanks (Fig. 10). Kirchhoff's equation for the current in the n-th element looks as

$$\left(i\omega C+\frac{1}{i\omega L}+G\right)\cdot V_n+i\omega\, C_c(V_{n-1}+V_{n+1})=0, \tag{6}$$

where C, L, and G are the capacitance, inductance, and conductance of the tank, C_c is the coupling capacitance, and V_i is the voltage on the i-th tank.

The dispersion equation is

$$i\omega C+\frac{1}{i\omega L}+G-2i\omega C_c\ \cos ka=0 \tag{7}$$

with $k=\beta-i\alpha$ followed by

$$\omega=\frac{\omega_0}{\sqrt{1+K_c\ \cos\ \beta a}}\quad \text{and}\quad \alpha\cdot a=\frac{1}{QK_c\ \sin\ \beta a}. \tag{8}$$

Here $K_c=2C_c/C$ is the coupling coefficient, $\omega_0=1/\sqrt{LC}$ and $Q=\omega_0 C/G$ are the resonant frequency and the Q-factor of the tank. Actually the LC-parameters of the resonant spherical particles are unknown, so we use the presented approach only for a qualitative description of the dispersion inside the chain. As in the case of magneto-inductive waveguide, the stop-bands occur and the backward wave can be observed in the 1D structure. The magnetic field distribution in the 1D structure for different moments of the period of the electromagnetic wave demonstrates the backward wave propagation (Fig. 11).

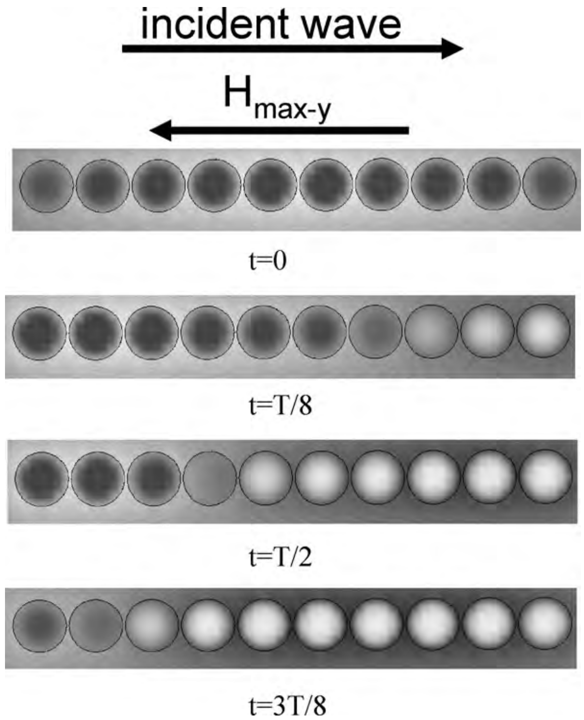

Fig. 11. The magnetic field distribution in the 1D structure of coupled resonant spherical particles for different moments of the time period.

The 2D plane structure consisting of 24 closely positioned dielectric spheres has been modeled. If the distance between the spheres is large, there is no wave propagation at the resonant frequency (Fig. 12a). By decreasing the spacing between the spheres, the splitting of the resonance curve occurs (Fig. 12b) and the pass band appears near the resonant frequency. Fig. 13 represents the phase diagram of the structure considered. The transverse magnetic field component in the free space is shown at the left side of the picture. The right side represents the magnetic field pattern for the structure containing the regular array of dielectric spheres. It is clearly seen from the magnified part of the picture that the phase response of the propagated electromagnetic inside the array of the spheres is positive, whereas the phase response outside the structure is negative. That means backward wave propagation in the structure is considered. Backward wave existence is explained

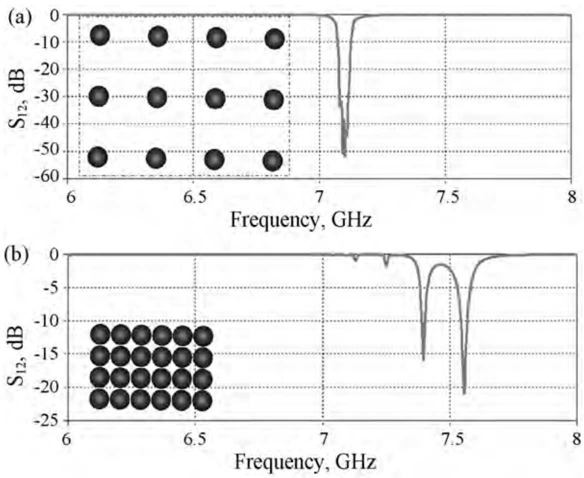

Fig. 12. Transmission coefficient of weakly (a) and strongly (b) coupled dielectric resonators.

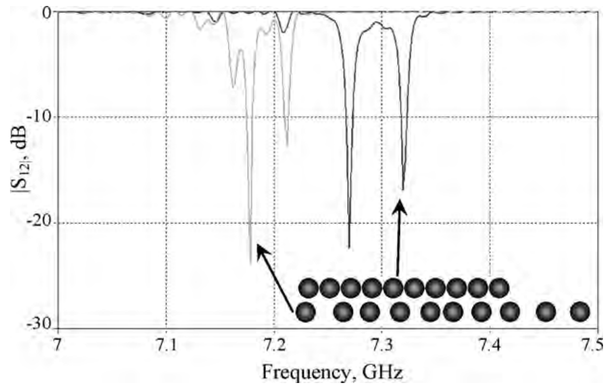

Fig. 14. Transmission coefficient versus frequency for a regular 1D structure of coupled resonant spheres (red line) and for randomly distributed spheres (grey line).

by a strong spatial dispersion in the chain of coupled dielectric spheres. The dispersion leads to disturbing the isotropy of the new structure. In this case backward wave can be observed only in the directions parallel to the crystallographic axes of the structure. But cubic symmetry and the symmetry of spherical particles let us expect that there will not be a strong dependence of the artificial material properties on the direction of wave incidence.

Important subject is the practical realization of the 3D isotropic structure. From this point of view, it is useful to analyze how the properties of the medium are changed, if the regular structure is replaced by randomly distributed interacting spherical resonators. As an example, the one-dimensional structure of strongly coupled dielectric resonators is considered. The results of a simulation of the transmission coefficient of a regular structure with spacing between resonators $s = 0.1$ mm in comparison with the results obtained for the same resonators with randomly distributed spacings $s = 0.1–2$ mm are shown in Fig. 14. In principle, the result remains the same: the resonance response of the single sphere is split. The observed shift to the lower frequencies is mainly caused by higher values of the spacing used in the random structure. Hence, the 3D isotropic DNG structure can be fabricated as a structure with randomly positioned constituent particles.

In case of the volumetric structure arranged in the simple cubic symmetry as 3D closely positioned spher-

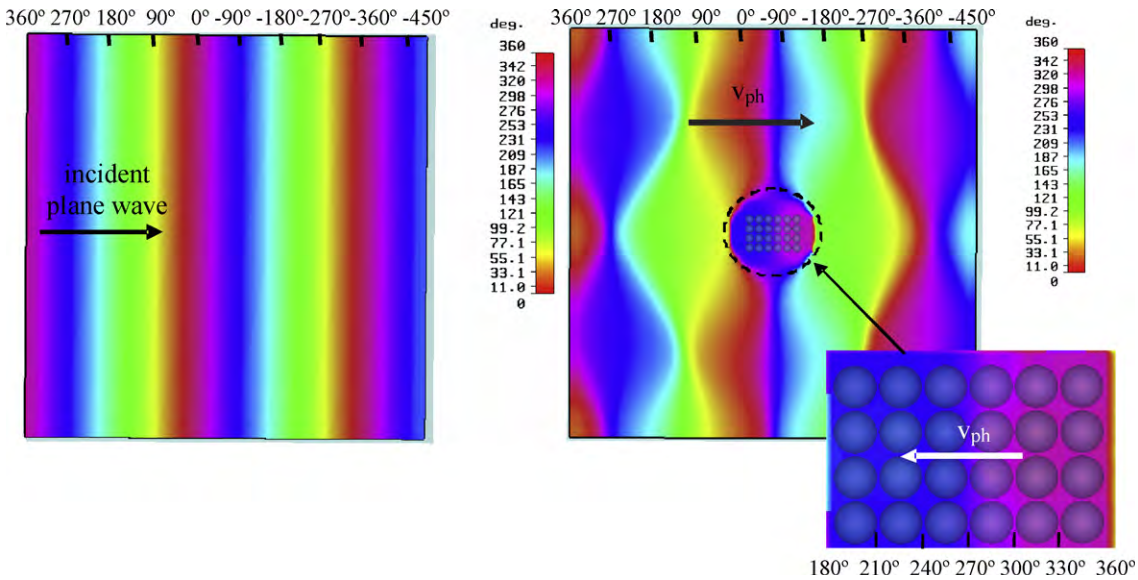

Fig. 13. The phase response of the array of 24 strongly coupled dielectric spherical resonators.

ical resonant dielectric particles, the DNG behavior is expected. The isotropic DNG response is conditioned by the cubic symmetry of the structure.

4. Conclusions

A double negative artificial material based on bi-spherical dielectric spherical resonators has been investigated. In the case of distantly positioned particles when the interaction between particles can be neglected and the system behaves as a homogeneous one for the incident wave, the isotropy of the structure is expected. It is explained by the cubic symmetry of the lattice.

A new structure with a higher packing density has been introduced in order to strengthen the DNG effect. Strong spatial dispersion leads to a backward wave propagation inside this structure. This dispersion can disturb the isotropy. But cubic symmetry of the structure (in the case of three-dimensional) as well as spherical shape of the constituent particles allows to expect close to isotropic properties of the artificial material. Backward wave existence in the new structure has been confirmed by numerical analysis. A conception of the new type of metamaterial based on electrically coupled resonators was introduced. Simulation results revealed the DNG behavior in 1D and 2D structures based on coupled dielectric resonators.

Acknowledgment

Discussions of the problem on workshops of VI “Metamorphose” are greatly appreciated.

References

[1] Th. Koschny, L. Zhang, C.M. Soukoulis, Isotropic three-dimensional left-handed metamaterials, Phys. Rev. B71 (2005) 121103.

[2] I. Jelinek, R. Marques, F. Mesa, J.D. Baena, Periodic arrangements of chiral scatterers providing negative refractive index bi-isotropic media, Phys. Rev. B 77 (2008) 205110.

[3] J. Zehentner, J. Machac, Volumetric single negative metamaterials, in: Proceedings of Metamaterials 2007 Congress, Rome, 22–24 October, 2007, pp. 617–620.

[4] A. Alu, N. Engheta, Three-dimensional nanotransmission lines at optical frequencies: a recipe for broad-band negative-refraction optical metamaterials, Phys. Rev. B 75 (2007) 024304.

[5] R. Simovski, S.A. Tretyakov, Model of isotropic resonant magnetism in the visible range based on core-shell clusters, Phys. Rev. B 79 (2009) 045111.

[6] C. Holloway, E. Kuester, A double negative composite medium composed of magnetodielectric spherical particles embedded in a matrix, IEEE Trans. AP 51 (2003) 2596.

[7] O.G. Vendik, M.S. Gashinova, Artificial double negative (DNG) media composed by two different dielectric sphere lattices embedded in a dielectric matrix, in: Proceedings of European Microwave Conference EuMC34, 1209, Paris, France, 2004.

[8] I. Vendik, O. Vendik, M. Gashinova, Artificial dielectric medium possessing simultaneously negative permittivity and magnetic permeability, Tech. Phys. Lett. 32 (2006) 429.

[9] I. Vendik, O. Vendik, I. Kolmakov, M. Odit, Modeling isotropic DNG media for microwave applications, Opto-Electron. Rev. 14 (2006) 179.

[10] M. Odit, I. Vendik, O. Vendik, 3D Isotropic metamaterial based on dielectric resonant spheres, in: Proceedings of Metamaterials 2007, 946, Rome, Italy, 2007.

[11] P. Alitalo, S. Maslovski, S. Tretyakov, Three-dimensional isotropic perfect lens based on LC-loaded transmission lines, J. Appl. Phys. 99 (2006) 064912.

[12] A. Ahmadi, H. Mosallaei, Physical configuration and performance modeling of all-dielectric metamaterials, Phys. Rev. B 77 (2008) 045104.

[13] E.A. Semouchkina, G.B. Semouchkin, M. Lanagan, C.A. Randall, FDTD study of resonance processes in metamaterials, IEEE Trans. Microwave Theory Tech. 53 (2005) 1477.

[14] T. Ueda, A. Lail, T. Itoh, Negative refraction in a cut-off parallel-plate waveguide loaded with two-dimensional lattice of dielectric resonators, in: Proceedings of European Microwave Conference EuMC36, 2005, p. 435.

[15] Qian Zhao, Lei Kang, B. Du, H. Zhao, Q. Xie, X. Huang, B. Li, J. Zhou, L. Li, Experimental demonstration of isotropic negative permeability in a three-dimensional dielectric composite, Phys. Rev. Lett. 101 (2008) 027402.

[16] K. Shibuya, K. Takano, N. Matsumoto, K. Izumi, H. Miyazaki, Y. Jimba, M. Hangyo, Terahertz metamaterials composed of TiO_2 cube arrays, in: Proceedings of the Metamaterial, 777, Pamplona, Spain, 2009.

[17] X. Cai, Z. Rui, G. Hu, Experimental study for metamaterials based on dielectric resonators and wire frame, Metamaterials 2 (4) (2008) 220–226.

[18] J.F. Nye, Physical Properties of Crystals, Oxford at the Clarendon Press, 1964.

[19] E.A. Nenasheva, N.F. Kartenko, O.N. Trubitsina, V.F. Matveichuk, S.N. Sibirtsev, I.M. Gaidamaka, Tunability and microwave dielectric properties of $BaO–SrO–Nd_2O_3–TiO_2$ ceramics, J. Eur. Ceram. Soc. 27 (2007) 2845–2848.

[20] E. Shamonina, V.A. Kalinin, K.H. Ringhofer, L. Solymar, Magneto-inductive waveguide, Electron. Lett. 38 (2002) 371.

[21] E. Shamonina, V.A. Kalinin, K.H. Ringhofer, L. Solymar, Magnetoinductive waves in one, two, and three dimensions, J. Appl. Phys. 92 (2002) 6252.